J|A|C|S ARTICLES

Published on Web 09/23/2010

Paramagnetic Intermediates of (*E*)-4-Hydroxy-3-methylbut-2-enyl Diphosphate Synthase (GcpE/IspG) under Steady-State and Pre-Steady-State Conditions

Weiya Xu,[†] Nicholas S. Lees,[‡] Dolapo Adedeji,[†] Jochen Wiesner,[§] Hassan Jomaa,[§] Brian M. Hoffman,[‡] and Evert C. Duin*[,†]

Department of Chemistry and Biochemistry, Auburn University, Auburn, Alabama 36849, Department of Chemistry, Northwestern University, Evanston, Illinois 60208, and Institut für Klinische Chemie und Pathobiochemie, Universitätsklinikum Giessen und Marburg, D-Giessen, 35392 Giessen, Germany

Received March 2, 2010; E-mail: duinedu@auburn.edu

Abstract: (*E*)-4-Hydroxy-3-methylbut-2-enyl diphosphate synthase (GcpE/IspG) converts 2-*C*-methyl-D-erythritol-2,4-cyclodiphosphate (MEcPP) into (*E*)-4-hydroxy-3-methyl-but-2-enyl diphosphate (HMBPP) in the penultimate step of the methyl-erythritol phosphate (MEP) pathway for isoprene biosynthesis. MEcPP is a cyclic compound and the reaction involves the opening of the ring and removal of the C3 hydroxyl group consuming a total of two electrons. The enzyme contains a single [4Fe-4S] cluster in its active site. Several paramagnetic species are observed in steady-state and pre-steady-state kinetic studies. The first signal detected is from a transient species that displays a rhombic electron paramagnetic resonance (EPR) signal with $g_{xyz} = 2.000$, 2.019, and 2.087 (FeS_A). A second set of EPR signals (FeS_B) accumulated during the reaction. Labeling studies with ^{57}Fe showed that all species observed are iron−sulfur-based. ^{31}P-ENDOR measurements on the FeS_A species showed a weak ^{31}P coupling which is in line with binding of the substrate to the enzyme in close proximity of the active-site cluster. On the basis of the EPR/ENDOR measurements, we propose a direct binding of the substrate to the [4Fe−4S] cluster during the reaction, and therefore that the iron−sulfur cluster is directly involved in a reductive elimination of a hydroxyl group. The FeS_B signal also showed ^{31}P coupling; in this case, however, it could be shown that the signal is due to the binding of the reaction product HMBPP to the active site cluster.

Introduction

In nature, there are two pathways found for the synthesis of the precursors isopentenyl pyrophosphate (IPP) and dimethylallyl pyrophosphate (DMAPP), which are the building blocks for the large group of essential biological molecules called isoprenoids, which include vitamins, cholesterol, steroid hormones, carotenoids, and quinones.[1,2] Mammals use the mevalonate pathway to synthesize the isoprene precursors, while eubacteria and apicomplexan parasites use the methyl-erythritol phosphate (MEP) pathway as the sole pathway for isoprene synthesis.[1] Several of the microorganisms that depend on the MEP pathway are pathogens, causing, for example, malaria, tuberculosis, anthrax, plague, gastrointestinal ulcers, and venereal diseases.[3] This makes the MEP pathway an attractive target for the development of new anti-infective drugs. Since this pathway is not present in humans, these inhibitors should demonstrate very low toxicity.

Fosmidomycin and its derivatives are the only known compounds that target the MEP pathway by inhibition of the enzyme 1-deoxy-D-xylulose 5-phosphate reductoisomerase (Figure 1).[4−7] Patients suffering from acute uncomplicated *Plasmodium falciparum* infections could be successfully treated with fosmidomycin, but an overall cure rate of 95% in clinical studies was only achieved when fosmidomycin was tested in combination with clindamycin.[4,5,8−10] Research efforts focus on finding fosmidomycin analogues that can work as stand-alone drugs[11−19] but also on finding inhibitors for the other enzymes in the MEP pathway, which when used in combination with fosmidomycin

[†] Auburn University.
[‡] Northwestern University.
[§] Universitätsklinikum Giessen und Marburg.

(1) Rohmer, M. *Nat. Prod. Rep.* **1999**, *16*, 565–574.
(2) Eisenreich, W.; Bacher, A.; Arigoni, D.; Rohdich, F. *Cell. Mol. Life Sci.* **2004**, *61*, 1401–1426.
(3) Rohdich, F.; Bacher, A.; Eisenreich, W. *Biochem. Soc. Trans.* **2005**, *33*, 785–791.
(4) Kuzuyama, T.; Shimizu, T.; Takahashi, S.; Seto, H. *Tetrahedron Lett.* **1998**, *39*, 7913–7916.
(5) Zeidler, J.; Schwender, J.; Muller, C.; Wiesner, J.; Weidemeyer, C.; Beck, E.; Jomaa, H.; Lichtenthaler, H. K. *Z. Naturforsch.* **1998**, *53c*, 980–986.
(6) Jomaa, H.; Wiesner, J.; Sanderbrand, S.; Altincicek, B.; Weidemeyer, C.; Hintz, M.; Turbachova, I.; Eberl, M.; Zeidler, J.; Lichtenthaler, H. K.; Soldati, D.; Beck, E. *Science* **1999**, *285*, 1573–1576.
(7) Koppisch, A. T.; Fox, D. T.; Blagg, B. S. J.; Poulter, D. C. *Biochemistry* **2002**, *41*, 236–243.
(8) Missinou, M. A.; Borrmann, S.; Schindler, A.; Issifou, S.; Adegnika, A. A.; Matsiegui, P.-B.; Binder, R.; Lell, B.; Wiesner, J.; Baranek, T.; Jomaa, H.; Kremsner, P. G. *Lancet* **2002**, *360*, 1941–1942.
(9) Lell, B.; Ruangweerayut, R.; Wiesner, J.; Missinou, M. A.; Schindler, A.; Baranek, T.; Hintz, M.; Hutchinson, D.; Jomaa, H.; Kremsner, P. G. *Antimicrob. Agents Chemother.* **2003**, *47*, 735–738.

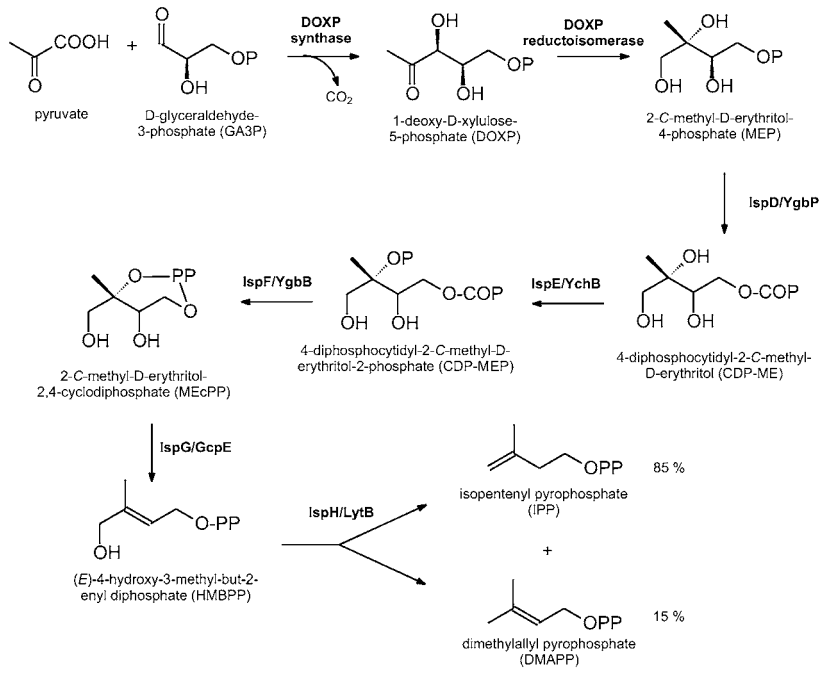

Figure 1. The MEP pathway for isoprene synthesis (P = phosphate).

are expected to show a pronounced synergistic increase in efficacy. Since many isoprenoids have biotechnological applications as drugs, flavors, pigments, perfumes, or agrochemicals, detailed knowledge of the mechanisms of the enzymes and regulation of the pathway could benefit the biotechnological production of commercially interesting isoprenoids, such as carotenoids.[20,21] The MEP pathway is also present in the plastids of plants, and targeting this pathway could result in the development of novel herbicides that are less harmful to humans.[22,23]

(*E*)-4-Hydroxy-3-methylbut-2-enyl diphosphate synthase (also called GcpE or IspG) (Figure 1) is the enzyme that catalyzes the penultimate step in the MEP pathway, the conversion of 2-*C*-methyl-D-erythritol-2,4-cyclodiphosphate (MEcPP) into (*E*)-4-hydroxy-3-methylbut-2-enyl diphosphate (HMBPP).[24−28] The reaction requires two electrons which can be provided in vitro by the artificial reductant dithionite.[25,29]

GcpE is an iron−sulfur-cluster-containing protein. Sequence alignments show that there are just three highly conserved cysteine residues present, which means that only one cluster can be coordinated to the protein.[29−31] Still, different cluster types have been detected in GcpE from different sources, and even the same source, including [2Fe−2S], [3Fe−4S], and [4Fe−4S] clusters.[31,32] Recently, we showed that purification of the enzyme from *Thermus thermophilus* under exclusion of

(10) Borrmann, S.; Issifou, S.; Esser, G.; Adegnika, A. A.; Ramharter, M.; Matsiegui, P. B.; Oyakhirome, S.; Mawili-Mboumba, D. P.; Missinou, M. A.; Kun, J. F. J.; Jomaa, H.; Kremsner, P. G. *J. Infect. Dis.* **2004**, *190*, 1534–1540.
(11) Giessmann, D.; Heidler, P.; Haemers, T.; Van Calenbergh, S.; Reichenberg, A.; Jomaa, H.; Weidemeyerd, C.; Sanderbrand, S.; Wiesner, J.; Link, A. *Chem. Biodivers.* **2008**, *5*, 643–656.
(12) Haemers, T.; Wiesner, J.; Giessmann, D.; Verbrugghen, T.; Hillaert, U.; Ortmann, R.; Jomaa, H.; Link, A.; Schlitzer, M.; Van Calenbergh, S. *Bioorg. Med. Chem.* **2008**, *16*, 3361–3371.
(13) Wiesner, J.; Ortmann, R.; Jomaa, H.; Schlitzer, M. *Archiv Pharm.* **2007**, *340*, 667–669.
(14) Ortmann, R.; Wiesner, J.; Silber, K.; Klebe, G.; Jomaa, H.; Schlitzer, M. *Archiv Pharm.* **2007**, *340*, 483–490.
(15) Devreux, V.; Wiesner, J.; Jomaa, H.; Van der Eycken, J.; Van Calenbergh, S. *Bioorg. Med. Chem. Lett.* **2007**, *17*, 4920–4923.
(16) Devreux, V.; Wiesner, J.; Jomaa, H.; Rozenski, J.; Van der Eycken, J.; Van Calenbergh, S. *J. Org. Chem.* **2007**, *72*, 3783–3789.
(17) Haemers, T.; Wiesner, J.; Busson, R.; Jomaa, H.; Van Calenbergh, S. *Eur. J. Org. Chem.* **2006**, 3856–3863.
(18) Devreux, V.; Wiesner, J.; Goeman, J. L.; Van der Eycken, J.; Jomaa, H.; Van Calenbergh, S. *J. Med. Chem.* **2006**, *49*, 2656–2660.
(19) Haemers, T.; Wiesner, J.; Van Poecke, S.; Goeman, J.; Henschker, D.; Beck, E.; Jomaa, H.; Van Calenbergh, S. *Bioorg. Med. Chem. Lett.* **2006**, *16*, 1888–1891.
(20) Matthews, P. D.; Wurtzel, E. T. *Appl. Microbiol. Biotechnol.* **2000**, *53*, 396–400.
(21) Rodríguez-Concepción, M.; Querol, J.; Lois, L. M.; Imperial, S.; Boronat, A. *Planta* **2003**, *217*, 476–482.
(22) Lichtenthaler, H. K.; Zeidler, J.; Schwender, J.; Muller, C. *Z. Naturforsch. C: Biosci.* **2000**, *55*, 305–313.
(23) Fellermeier, M.; Kis, K.; Sagner, S.; Maier, U.; Bacher, A.; Zenk, M. H. *Tetrahedron Lett.* **1999**, *40*, 2743–2746.
(24) Hecht, S.; Eisenreich, W.; Adam, P.; Amslinger, S.; Kis, K.; Bacher, A.; Arigoni, D.; Rohdich, F. *Proc. Natl. Acad. Sci. U.S.A.* **2001**, *98*, 14837–14842.
(25) Kollas, A.-K.; Duin, E. C.; Eberl, M.; Altincicek, B.; Hintz, M.; Reichenberg, A.; Henschker, D.; Henne, A.; Steinbrecher, I.; Ostrovsky, D. N.; Hedderich, R.; Beck, E.; Jomaa, H.; Wiesner, J. *FEBS Lett.* **2002**, *532*, 432–436.
(26) Wolff, M.; Seemann, M.; Grosdemange-Billiard, C.; Tritsch, D.; Campos, N.; Rodríguez-Concepción, M.; Boronat, A.; Rohmer, M. *Tetrahedron* **2002**, *43*, 2555–2559.
(27) Seemann, M.; Campos, N.; Rodríguez-Concepción, M.; Ibañez, E.; Duvold, T.; Tritsch, D.; Boronat, A.; Rohmer, M. *Tetrahedron* **2002**, *43*, 1413–1415.
(28) Rohdich, F.; Zepeck, F.; Adam, P.; Hecht, S.; Kaiser, J.; Laupitz, R.; Gräwert, T.; Amslinger, S.; Eisenreich, W.; Bacher, A.; Arigoni, D. *Proc. Natl. Acad. Sci. U.S.A.* **2003**, *100*, 1586–1591.
(29) Adedeji, D.; Hernandez, H.; Wiesner, J.; Köhler, U.; Jomaa, H.; Duin, E. C. *FEBS Lett.* **2007**, *581*, 279–283.
(30) Altincicek, B.; Kollas, A.-K.; Sanderbrand, S.; Wiesner, J.; Hintz, M.; Beck, E.; Jomaa, H. *J. Bacteriol.* **2001**, *183*, 2411–2416.
(31) Seemann, M.; Wegner, P.; Schünemann, V.; Tse Sum Bui, B.; Wolff, M.; Marquet, A.; Trautwein, A.; Rohmer, M. *J. Biol. Inorg. Chem.* **2005**, *10*, 131–137.
(32) Okada, K.; Hase, T. *J. Biol. Chem.* **2005**, *280*, 20672–20679.

oxygen resulted in an active enzyme preparation that solely contained 4Fe clusters.[29] The cluster showed the unusual property that it cannot be reduced by dithionite in the absence of substrate, while incubation with the stronger reductant titanium(III) citrate resulted in the breakdown of the cluster. This required the use of a combination of electron paramagnetic resonance (EPR) and magnetic circular dichroism spectroscopy to confirm the absence of a $[3Fe-4S]^{+}$ cluster and resonance Raman spectroscopy to confirm the presence of a $[4Fe-4S]^{2+}$ cluster.[29] The purified protein contained 3.9 mol of Fe per mol of enzyme indicating that close to 100% of the enzyme molecules contained this type of cluster.

In kinetic studies when GcpE was incubated with both dithionite and MEcPP, a transient paramagnetic species was detected by EPR spectroscopy that was assigned to an iron−sulfur-cluster-bound reaction intermediate.[29] Here data will be presented to show that this species represents a true reaction intermediate. Enzyme purified from cells grown on ^{57}Fe displayed a broadening of the EPR signal indicating that it is in large part iron−sulfur based. Additional spectroscopic data are presented on several other iron−sulfur-based species that are detected during the kinetic studies. A hypothetical reaction mechanism and the relevance of these species to this mechanism will be discussed. With the reaction requiring two electrons and the ability of the cluster to donate only one electron at-a-time, a radical mechanism was expected for this enzyme and several examples of this type of mechanism have been proposed in the literature.[2,24,25,28,33] Our data, however, suggests that this may not be the case. We propose that instead the enzyme forms a cluster-stabilized reaction intermediate similar to that observed in ferredoxin:thioredoxin reductase (FTR).[34−38] Formation of this species allows the reaction to proceed without formation of a highly reactive radical species.

Methods and Materials

Elemental ^{57}Fe (95% enrichment) was from WEB Research Co. $^{57}FeCl_3$ was prepared by reacting solid ^{57}Fe in 37% HCl. After all iron reacted, the pH was adjusted to 4−5 with NaOH. Ti(III) citrate (200 mM) was prepared from $TiCl_3$ (Fluka) in 250 mM sodium citrate under strictly anaerobic conditions. The pH of the solution was adjusted to 7.0 with sodium hydrogen carbonate. The substrate MEcPP was isolated from *Corynebacterium ammoniagenes*.[25] All gases and gas mixtures were from Airgas.

Expression and Purification of GcpE. Plasmids containing the *gcpE* gene from *T. thermophilus* were used to transform *Escherichia coli* XL1-Blue cells (Stratagene).[25] The expression of the *gcpE* gene is controlled by the lac promoter, and the expression of the GcpE protein was induced by the addition of isopropyl-1-thio-β-D-galactopyranoside. Routinely, cells are cultivated with aeration at 37 °C in 1-L SOC medium (20.0 g of tryptone, 5.0 g of yeast extract, 8.6 mM NaCl, 10 mM $MgCl_2$, 10 mM $MgSO_4$, and 20 mM glucose) supplemented with ampicillin (25 μg mL^{-1}) and $FeCl_3$ (100 μM). For the isotopic enrichment with ^{57}Fe, 100 μM $^{57}FeCl_3$ was used.

All purification steps and subsequent sample handling were carried out in a Coy glovebox under an atmosphere of N_2/H_2 (95%/5%) with dioxygen-free solutions as described earlier.[25,29] Cells from a 1-L culture were gathered by centrifugation, frozen, and stored at −80 °C until use. In the first step of the purification procedure, the cells were resuspended in 20 mM Tris-HCl (pH 8.0) and were disintegrated by sonication, followed by a centrifugation step. The supernatant was then subjected to denaturation at a heat of 65 °C for 30 min. The protein was further purified using two column separation steps, first a diethylaminoethyl (DEAE) Sepharose column (GE Healthcare), and subsequently, a MonoQ column (GE Healthcare). The main fractions, as detected on SDS−PAGE (42 kDa), were collected and concentrated using a Centricon YM-30 centrifugal filter device (Millipore). Generally, 25 mg of protein is produced following these procedures. The purified protein was directly used or stored at −80 °C until further use. Removal of adventitiously bound product, HMBPP, was performed by running the protein solution over a PD10 desalting column (GE Healthcare).

Determination of Protein Concentration and Fe Content. Enzyme concentration was determined by the method of Bradford.[39] For the iron determination, protein samples were passed over Chelex 100 (Bio-Rad) to remove adventitiously bound iron. Iron was determined using a rapid ferrozine-based colorimetric method.[40]

Kinetic Studies. A colorimetric assay was used to obtain kinetic parameters.[41,42] The starting solution contained GcpE, dithionite, and the redox dye methyl viologen (Aldrich), which has a blue color when reduced. The activity was determined by measuring the absorbance change at 603 nm as a function of time.

The apparatus and procedures for preparation of freeze-quenched samples have been described.[43,44] Two syringes were filled under exclusion of molecular oxygen inside a glovebox. One syringe contained the GcpE enzyme and the dithionite. The other syringe contained the substrate solution. See the figures for the final concentration of each component after mixing. A similar approach was followed when the samples were mixed and incubated by hand. In the latter case, the samples were flash-frozen in the Coy box in cold ethanol (200 K).

When methyl viologen was used as the sole reductant, the compound was reduced by adding dithionite in a concentration less than half the methyl viologen concentration. Dithionite provides two electrons and by adding less than half the methyl viologen concentration no reduced dithionite is present.

Spectroscopic Measurements. EPR spectra at X-band frequency (9 GHz) were obtained with a Bruker EMX spectrometer fitted with the ER-4119-HS high sensitivity perpendicular-mode cavity or the ER-4116-DM dual-mode cavity. Cooling of the sample was performed with an Oxford Instruments ESR 900 flow cryostat with an ITC4 temperature controller or with a liquid-nitrogen finger Dewar.

Spin quantization was carried out under nonsaturating conditions using 10 mM copper perchlorate as the standard (10 mM $CuSO_4$, 2 mM $NaClO_4$, 10 mM HCl). Signal intensity is presented as spin, the fraction of EPR signal intensity with respect to the amount of [4Fe−4S] cluster present in the sample: 1 spin is 100% signal

(33) Brandt, W.; Dessoy, M. A.; Fulhorst, M.; Gao, W.; Zenk, M. H.; Wessjohann, L. A. *ChemBioChem* **2004**, *5*, 311–323.
(34) Staples, C. R.; Ameyibor, E.; Fu, W.; Gardet-Salvi, L.; Stritt-Etter, A.-L.; Schürmann, P.; Knaff, D. B.; Johnson, M. K. *Biochemistry* **1996**, *35*, 11425–11434.
(35) Staples, C. R.; Gaymard, E.; Stritt-Etter, A.-L.; Telser, J.; Hoffman, B. M.; Schürmann, P.; Knaff, D. B.; Johnson, M. K. *Biochemistry* **1998**, *37*, 4612–4620.
(36) Dai, S.; Schwendtmayer, C.; Schürmann, P.; Ramaswamy, S.; Eklund, H. *Science* **2000**, *287*, 655–658.
(37) Jameson, G. N. L.; Walters, E. M.; Manieri, W.; Schürmann, P.; Johnson, M. K.; Huynh, B. H. *J. Am. Chem. Soc.* **2003**, *125*, 1146–1147.
(38) Walters, E. M.; Garcia-Serres, R.; Jameson, G. N. L.; Glauser, D. A.; Bourquin, F.; Manieri, W.; Schürmann, P.; Johnson, M. K.; Huynh, B.-H. *J. Am. Chem. Soc.* **2005**, *127*, 9612–9624.
(39) Bradford, M. M. *Anal. Biochem.* **1976**, *72*, 248–254.
(40) Fish, W. W. *Methods Enzymol.* **1988**, *158*, 357–364.
(41) Altincicek, B.; Duin, E. C.; Reichenberg, A.; Hedderich, R.; Kollas, A.-K.; Hintz, M.; Wagner, S.; Wiesner, J.; Beck, E.; Jomaa, H. *FEBS Lett.* **2002**, *532*, 437–440.
(42) Röhrich, R. C.; Englert, N.; Troschke, K.; Reichenberg, A.; Hintz, M.; Seeber, F.; Balconi, E.; Aliverti, A.; Zanetti, G.; Köhler, U.; Pfeiffer, M.; Beck, E.; Jomaa, H.; Wiesner, J. *FEBS Lett.* **2005**, *579*, 6433–6438.
(43) Bollinger, J. M., Jr.; Tong, W. H.; Ravi, N.; Huynh, B.-H.; Edmondson, D. E.; Stubbe, J. *Methods Enzymol.* **1995**, *258*, 278–303.
(44) Ravi, N.; Bollinger, J. M., Jr.; Huynh, B.-H.; Edmondson, D. E.; Stubbe, J. *J. Am. Chem. Soc.* **1994**, *116*, 8807–8014.

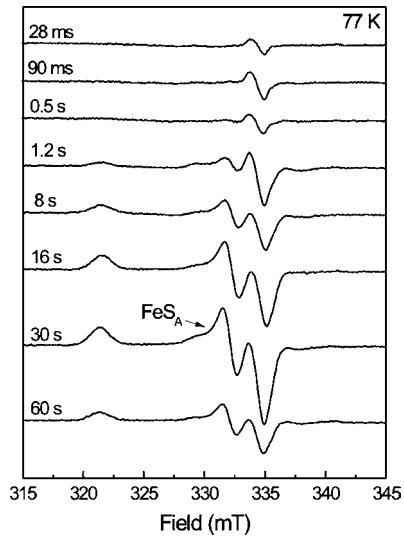

Figure 2. Electron paramagnetic resonance data for samples obtained with the freeze-quench technique in the presence of dithionite. After mixing each sample contained 0.4 mM GcpE, 5.5 mM MEcPP, and 25 mM dithionite in 100 mM TrisHCl, pH 8.0. Samples were mixed and incubated at RT. EPR conditions: microwave frequency, 9.385 GHz; microwave power incident to the cavity, 0.20 mW; field modulation frequency, 100 kHz; microwave amplitude, 0.6 mT; temperature 77 K.

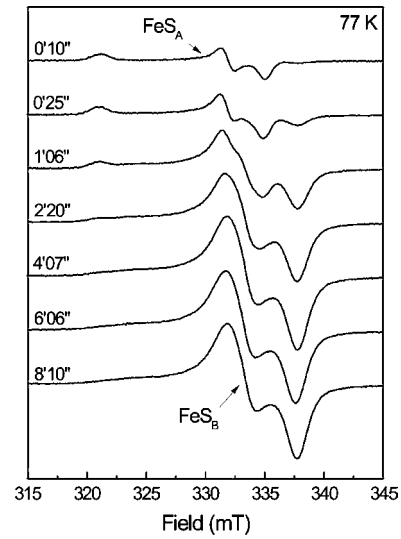

Figure 3. Electron paramagnetic resonance data for samples which were hand-mixed and flash frozen in the presence of dithionite. Samples were preincubated, mixed, and incubated at 55 °C. After mixing, each sample contained 0.10 mM GcpE, 4.0 mM MEcPP, and 15 mM dithionite in 100 mM TrisHCl, pH 8.0. For EPR conditions, see legend of Figure 2.

intensity. The software package developed by SPJ Albracht was used for computer simulations of the EPR signals.[45]

Pulsed EPR and ENDOR data (35 GHz and 2 K) were obtained with an instrument described earlier.[46,47]

Results

Kinetic Studies of Enzymatic Turnover. Our initial experiments were guided by the kinetic parameters obtained in the colorimetric assays, in the presence of methyl viologen. The maximal specific activity measured at RT for the GcpE enzyme is 0.124 μmol min^{-1} mg^{-1} at pH 8.0. The K_m value for MEcPP is 8.0 μM. A k_{cat} value of 0.09 s^{-1} was calculated which means that at RT one reaction cycle takes about 11 s. For a full conversion of MEcPP into HMBPP, however, the presence of only the artificial electron donor dithionite is sufficient,[25] and therefore methyl viologen was left out in the initial studies since it is EPR-active making the observation of other signals more difficult.

To have any chance of detecting a reaction intermediate, it should be detectable under steady-state conditions, using an excess of dithionite and substrate. Under these conditions, the first part of the process, up to 11 s, should present the pre-steady-state phase followed by the steady-state phase. The first set of data is from a rapid-mix/rapid-freeze experiment where a solution containing GcpE and dithionite was rapidly mixed with a solution containing MEcPP. The reaction was allowed to proceed for a set amount of time after which the reaction was halted by rapid freezing of the reaction mixture. The EPR spectra obtained for the different samples are shown in Figure 2. From 28 ms to 0.5 s, the main signal detected was an isotropic EPR signal with $g_{iso} = 2.005$. At 1.2 s, a new, more rhombic EPR signal (designated FeS$_A$) with $g_{xyz} = 2.000$, 2.019, and 2.087 started to develop. The intensity of this signal reached a maximum value at 30 s. At 60 s, the signal intensity decreased again. The maximal EPR signal intensity of this species ranged from about 0.05 to as high as 0.20 spin in different experiments.

The spectra shown in Figure 2 were measured at 77 K. Measurements at other temperatures showed that these are the only paramagnetic species present in these samples. For example, signals with properties typical of $[4Fe-4S]^+$ clusters (perpendicular mode) or of $[3Fe-4S]^0$ clusters (using parallel-mode EPR spectroscopy) were not detected (not shown). The samples that were frozen at 30 and 60 s showed small amounts of other paramagnetic species. These, however, are more clearly detectable in a different set of EPR spectra, as now discussed.

Figure 3 shows an additional set of kinetic data. In this case, the solution containing GcpE and dithionite and the solution containing MEcPP were incubated at 55 °C for various times then mixed by hand and flash frozen in cold ethanol (200 K). In the samples frozen after an incubation time of 10 and 25 s, the rhombic EPR signal belonging to the FeS$_A$ species can be detected. The 25 s sample, however, already shows the formation of an additional signal that reaches maximal intensity at 4 min and 7 s. This signal is not a transient signal since the intensity stays constant after the highest intensity is reached. This signal is stable for up to 16 min, the longest time the reaction mixtures were incubated (not shown). The maximal EPR signal intensity of this species can be as high as 0.4−0.5 spin. For the discussion here, we call this signal FeS$_B$. The signal, however, represents more than one paramagnetic species and has a very temperature-dependent appearance, detailed below. Note that the FeS$_B$ signal starts to develop faster at 55 °C due to a higher rate constant for the reaction, 0.6 μmol min^{-1} mg^{-1} at pH 8.0 (based on the colorimetric assay in the presence of methyl viologen).

The experiments in Figures 2 and 3 have been repeated several times under different conditions. In all cases, the same set of signals were detected: formation and disappearance of the FeS$_A$ species and accumulation of the FeS$_B$ species. The FeS$_B$ signal did not show differences in the development rate

(45) Beinert, H.; Albracht, S. P. J. *Biochim. Biophys. Acta* **1982**, *683*, 245–277.
(46) Davoust, C. E.; Doan, P. E.; Hoffman, B. M. *J. Magn. Reson.* **1996**, *A 119*, 38–44.
(47) Zipse, H.; Artin, E.; Wnuk, S.; Lohman, G. J. S.; Martino, D.; Griffin, R. G.; Kacprzak, S.; Kaupp, M.; Hoffman, B.; Bennati, M.; Stubbe, J.; Lees, N. *J. Am. Chem. Soc.* **2009**, *131*, 200–211.

of the different peaks in the EPR signal, indicating that although clearly more than one species is present, their kinetic behavior is identical (as are their EPR properties; see below). The signal intensity of either the FeS_A or the FeS_B species, however, is highly dependent on the concentration of MEcPP and dithionite used. For example, increasing the concentration of MEcPP from 0.5 to 3.0 mM more than doubles the signal intensity of the FeS_A signal (not shown). With concentrations of dithionite below 10 mM, the FeS_A species mainly accumulates. With concentrations of 15 mM and higher, the species behaves like a transient species. Assuming that the appearance and subsequent disappearance represent two independent redox processes, this might indicate a different midpoint potential or concentration dependency for the formation and breakdown of the FeS_A species. Increasing the temperature (RT vs 55 °C) also increases the signal intensity. When single-turnover experiments are performed (Figure S1, Supporting Information), the formation and breakdown of the different paramagnetic species are almost identical to that shown in Figures 2 and 3. The signal intensity of the FeS_A signal, however, reaches its maximal intensity within 10 s (at RT). The other signals still start to develop after about 1 min incubation time and accumulate over time. In single-turnover experiments, the EPR signal intensity of FeS_A is only 0.05 to 0.1 spin.

Because of the kinetic behavior of the two species, we assign the FeS_A signal to a reaction intermediate, while the FeS_B signal could be related to an end point in the conversion of MEcPP into HMBPP or a side reaction resulting in a dead-end product. Here we present data that this species is not a dead-end product. We previously reported that it was not possible to reduce the [4Fe−4S] cluster in substrate-free GcpE from *T. thermophilus*.[29] In a recent study by Liu and co-workers,[48] however, facile reduction with reduced methyl viologen was shown of the cluster of GcpE from *E. coli*. Therefore, the reduction of the cluster in our enzyme was reinvestigated. Reduction of the cluster with dithionite was detected, but in the *T. thermophilus* enzyme the amount of reduction is in the range of only 0.01−0.05 spin, which explains why this signal has been overlooked in our samples when using protein concentrations of 50−100 μM. Figure 4, trace A, shows the EPR spectrum of the reduced cluster obtained for the enzyme incubated with 10 mM dithionite. The enzyme was also treated with increasing amounts of reduced methyl viologen (reduced with dithionite). In this case, similar amounts of spin intensity for the reduced signal were detected when 1−2 equiv of methyl viologen was used with respect to the enzyme concentration. When higher amounts were used, the amount of reduction actually decreased (not shown). This seems to be in line with our previous studies that showed that incubation with the more potent reductant Ti(III) citrate does not result in higher amounts of cluster reduction but in slow breakdown of the iron−sulfur cluster.[29]

Some of the reduced protein samples showed a different EPR signal upon reduction (Figure 4, trace B) or a mixture of the two signals shown in Figure 4. This signal is identical to the low-temperature FeS_B signal detected in the kinetic studies (see below). It turned out that this FeS_B signal could only be detected in reduced GcpE samples if the enzyme was purified with a DEAE-Sepharose column that was used in several rounds of purification. With a freshly regenerated column, only spectrum A (Figure 4) is detected in the enzyme. Clearly something is

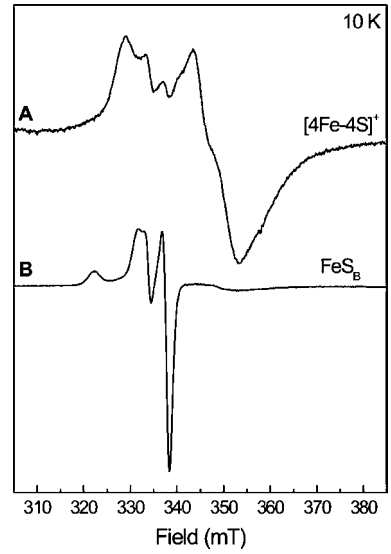

Figure 4. Electron paramagnetic resonance data for reduced GcpE samples. (A) Sample without adventitiously bound substrate HMBPP. The sample contained 1.3 mM GcpE and 10 mM dithionite. Signal intensity is 0.01 spin. (B) Sample with adventitiously bound HMBPP. The sample contained 0.5 mM GcpE and 10 mM dithionite. Signal intensity is 0.02 spin. EPR conditions for A and B: microwave frequency, 9.385 GHz; microwave power incident to the cavity, 2.0 mW; field modulation frequency, 100 kHz; microwave amplitude, 0.6 mT; temperature 10 K.

stuck to the enzyme causing the appearance of spectrum B (Figure 4). Enzyme preparations showing spectrum B can be converted into enzyme showing spectrum A by running the enzyme solution over a desalting PD10 column. The compound that is removed is probably the reaction product HMBPP since adding this compound to the enzyme preparations converted spectrum A into spectrum B (not shown). Therefore, it can be concluded that the FeS_B species is due to reduced enzyme with HMBPP bound.

To further prove that the FeS_B species does not represent a dead-end product, GcpE was incubated with both dithionite and MEcPP, and at different time intervals a sample was tested for activity in the colorimetric assay with methyl viologen and in parallel a sample was taken that was frozen for examination in EPR spectroscopy. This showed that the accumulation of the FeS_B signals is not accompanied by a significant loss of activity (not shown). This is in line with the assignment of a reduced enzyme with possibly bound reaction product. The fact that much more reduced cluster can be detected under these conditions could be because direct binding of HMBPP to the cluster has a significant effect on the midpoint potential of the cluster itself as seen in other enzymes.[49] The addition of the substrate MEcPP results in the replacement of the bound HMBPP and the next reaction cycle starts. This was confirmed by EPR studies where within 10−20 s after addition of MEcPP the FeS_A signal was detectable in addition to the FeS_B signal already present (not shown). This would indicate that HMBPP is a competitive inhibitor of GcpE.

The data in Figure 2 show the EPR spectra measured at 77 K. The samples have also been measured at 6 K to see if any additional signals due to reduced [4Fe−4S] can be detected. This is not the case, which could preclude a role for a $[4Fe-4S]^+$ form of the cluster. However, the work by Liu and co-workers

(48) Xiao, Y.; Zahariou, G.; Sanakis, Y.; Liu, P. *Biochemistry* **2010**, *48*, 10483–10485.

(49) Duin, E. C.; Madadi-Kahkesh, S.; Hedderich, R.; Clay, M. D.; Johnson, M. K. *FEBS Lett.* **2002**, *512*, 263–268.

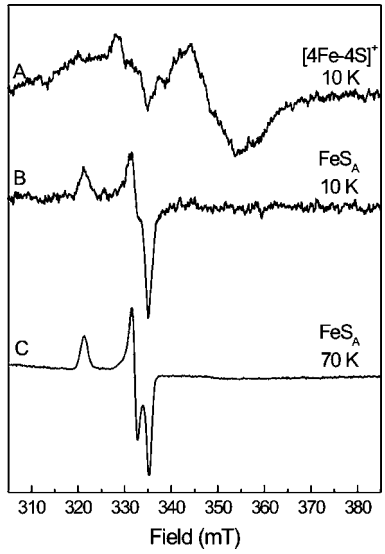

Figure 5. Electron transfer from reduced GcpE to MEcPP. The protein sample was incubated with 0.5 mM dithionite-reduced methyl viologen. The methyl viologen was removed by running the sample over a desalting column (PD10). (A) GcpE after desalting step. Sample measured at 10 K with a microwave power of 2.0 mW. (B) As A after addition of 10 mM MEcPP and incubation for 30 s before freezing. Sample measured at 10 K with a microwave power of 2.0 mW. **(**C) Same as B, measured at 70 K with a microwave power of 0.2 mW. The enzyme concentration is 53 μM in all samples. Signal intensity in A is 0.03 spin. In B, 0.10 spin. Note that these values probably do not indicate an increase in spin intensity. The uncertainty of the double-integration method is relatively large for very weak samples.

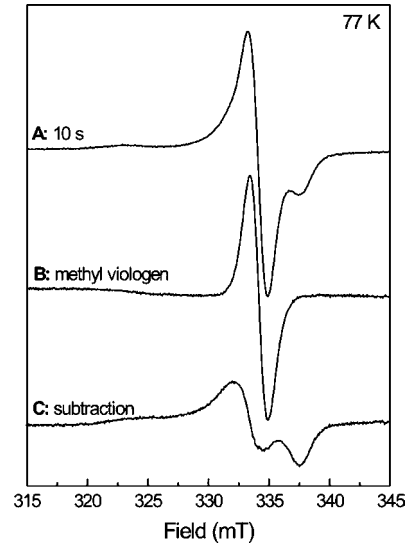

Figure 6. Electron paramagnetic resonance spectrum for a 10 s sample that was prepared in the presence of methyl viologen. Sample was preincubated, mixed, and incubated at RT. After mixing, the sample contained 1.1 mM GcpE, 10 mM MEcPP, 5 mM dithionite-reduced methyl viologen in 100 mM TrisHCl, pH 8.0. For EPR conditions see legend of Figure 2.

show that there is an optimal redox potential region for enzyme activity that seems to coincide with partial reduction of the active-site cluster. To test the involvement of the cluster, GcpE was incubated with an excess of reduced methyl viologen which was subsequently removed over an anaerobic PD10 desalting column. The complete removal of methyl viologen was checked in absorption spectroscopy. This procedure left some of the clusters present in the reduced form (Figure 5, trace A). The interesting part is that the reduced enzyme can only donate a total of one electron to the substrate which should result in the formation of the reaction intermediate. This was indeed the case. The addition of substrate to this enzyme preparation resulted in the loss of the 4Fe EPR signal (Figure 5, trace B) and the formation of the FeS_A signal (Figure 5, trace C). The signal detected in Figure 5, trace B, is due to the FeS_A species. At this temperature, however, the signal is highly saturated, in particular the g_y peak. Therefore, the same signal is also shown measured at a temperature of 70 K (Figure 5, trace C).

In the light of the k_{cat} values, the data are puzzling. In the freeze-quench experiment (Figure 2), we would expect to see a whole reaction cycle in the first 11 s (pre-steady-state) after which a equilibrium should be reached (steady state). Instead, the spectral changes take 60 s. Similar observations can be made for the single-turnover experiment (Figure S1, Supporting Information). In the last case, the spectral changes seem to continue past a full 3 min. It can be concluded that under the conditions used in the EPR experiments the reaction must be much slower and that the discrepancy between the kinetic parameters of the colorimetric assay and the EPR experiments must be due to the presence or absence of methyl viologen. Methyl viologen is widely used in enzymatic redox titrations as a redox mediator, enabling the easy transfer of electrons from the reductant to a metal center in a protein. When the reaction in the presence of methyl viologen was followed in EPR, a huge increase in the reaction speed was detected (Figure 6). Under these conditions, the FeS_A signal is not formed or only in very small amounts. Figure 6, trace A, shows the EPR spectrum of a sample frozen after 10 s of incubation time (RT). The presence in the EPR spectrum of an isotropic signal due to methyl viologen makes the formation of the GcpE signals more difficult to follow. Subtracting out the EPR signal due to methyl viologen (Figure 6, trace B) leaves a spectrum (Figure 6, trace C) identical to that of the FeS_B species (Figure 3). Before the experiment, it was made certain that this enzyme preparation did not show the FeS_B signal upon the addition of dithionite or reduced methyl viologen only. The addition of methyl viologen appears to increase the reaction rate by at least a factor 10.

Characterization of the Paramagnetic Species Present under Turnover Conditions by EPR and ENDOR Spectroscopies. EPR. The EPR signal of the FeS_A species shows remarkable similarities to an [4Fe−4S]-cluster-based EPR signal observed in FTR. The shape of the EPR signals in both enzymes shows resemblance to that of so-called high-potential iron−sulfur (HiPIP) clusters,[50] but HiPIP clusters are only detectable under highly oxidizing conditions. In addition, the temperature range in which the GcpE signal can be detected is very different from that of a HiPIP. Below 20 K, it is not possible to measure the GcpE signal in slow passage X-band measurements without saturation; from 20 to 100 K the signal can be measured, but without saturation. Above 100 K the signal starts to broaden and is broadened beyond detection at 160 K. A Curie plot can be found in the supplemental section (Figure S2, Supporting Information). This temperature behavior of the FeS_A signal is very similar to that of the signal detected in FTR.[35]

The temperature response of the FeS_B signal was also studied in more detail (Figure S3, Supporting Information). At 6 K, the dominant feature in the EPR spectrum is an axial signal with $g_{||} = 2.081$, $g_{\perp} = 1.984$ (Figure 7, trace B). A simulation

(50) Cammack, R.; Patil, D. S.; Fernandez, V. M. *Biochem. Soc. Trans.* **1985**, *13*, 572–578.

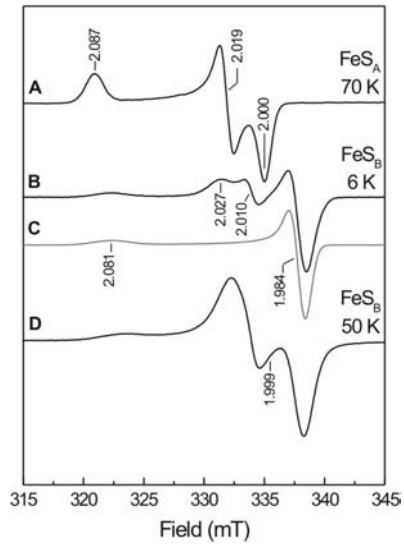

Figure 7. Overview of paramagnetic species detected in GcpE during turnover experiments. (A) FeS_A signal present in a sample incubated at 55 °C and frozen after 20 s. Contains 0.10 mM GcpE, 4.0 mM MEcPP, and 4.7 mM dithionite in 100 mM TrisHCl, pH 8.0. EPR conditions: microwave frequency, 9.385 GHz; microwave power incident to the cavity, 0.20 mW; field modulation frequency, 100 kHz; microwave amplitude, 0.6 mT; temperature, 70 K. (B) FeS_B signal present in sample incubated at 55 °C and frozen at 4 min and 7 s. Microwave power incident to the cavity, 2.0 μW; temperature, 6 K. (C) Simulation of axial component of B. Simulation parameters: $g_{\|} = 2.081$ and $g_{\perp} = 1.984$; $W_{\|} = 2.50$ mT and $W_{\perp} = 1.20$ mT. (D) Same as B but measured at 50 K, microwave power incident to the cavity, 2.0 mW.

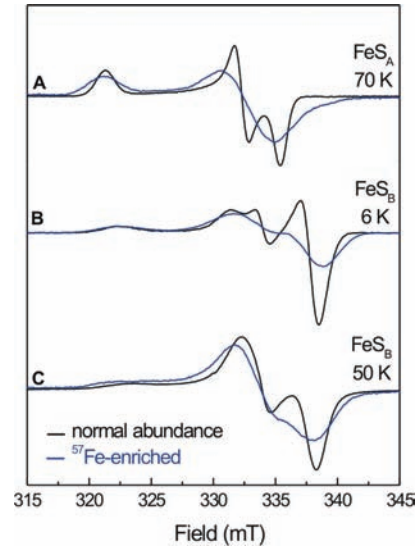

Figure 8. Overlay of the spectra from Figure 7 with similar samples prepared with ^{57}Fe-enriched enzyme (blue lines). Signal amplitudes were corrected for differences in sample concentration. For EPR conditions, see legend of Figure 7.

of this species has been included in Figure 7 (trace C) for assignment of this species in the original spectrum. Additional minority species also are present, with visible features including an edge at $g = 2.010$ and a maximum at 2.027. This spectrum, with the same relative proportions of contributing species, is observed for FeS_B (when FeS_A is not also present) in all preparations and under all spectrometer conditions, and the total spectrum is reproduced by the addition of product to the reduced enzyme, as described earlier. All of the signals thus involve product bound to the Fe cluster (see below). The relative intensity of the signals from FeS_B components is also invariant under a wide range of CW and pulsed EPR conditions, indicating extremely similar relaxation characteristics. With increasing temperature (Figure S3, Supporting Information), the low temperature spectrum starts to broaden and is no longer recognizable at 35−50 K. The 50 K spectrum (Figures S3 and 7, trace D) resembles a 2-fold split isotropic species, but due to the similar temperature behavior, it could be possible that the low field peak at 323 mT is part of this signal. It is not clear if the apparent shift in *g*-value observed for the peak at low field in traces B and D (Figure 7) is indicative for the presence of two different signals at 6 and 50 K or whether it is an artifact of the temperature broadening. As discussed below, this set of observations suggests that the multiple signals are associated with "valence isomers", a manifold of cluster states within a single cluster.

To test the assignment of the observed intermediate in the kinetic studies to a cluster-bound reaction intermediate, based on the similarities in EPR properties with a signal detected in FTR, enzyme was purified from cells that were fed ^{57}Fe-isotope in the form of $^{57}FeCl_3$. Enrichment with ^{57}Fe produced a considerable broadening of the EPR signal, which proves that the signal is iron−sulfur-cluster-based (Figure 8, trace A). Likewise, the set of FeS_B signals also shows this broadening of the EPR signal in ^{57}Fe-enriched enzyme (Figure 8, traces B and C). This occurs across the entire multicomponent EPR spectrum indicating that all species observed are iron−sulfur-cluster-based signals.

Several questions remain. The first one is the question of how the reaction intermediate is bound to the cluster. Second there is the question whether a radical species is formed that is stabilized or whether the enzyme is able to avoid forming a radical completely. There are several functional groups of MEcPP that could be involved in binding to the cluster. On the basis of the behavior of aconitase, the leaving hydroxyl group, and maybe also the other hydroxyl group, could bind to the unique iron in the 4Fe cluster. The phosphate groups would be less likely candidates, although a bond from a phosphate oxygen to an heme-iron ion is observed in sulfite reductase.[51] In a recent paper, Wang et al. were led by $^{13}C/^{17}O$ ENDOR/HYSCORE data to propose that the FeS_A intermediate represents a ferraoxetane structure, containing a direct Fe−C bond.[52]

ENDOR. Nonexchangeable Protons. The ^{1}H ENDOR of FeS_A/FeS_B in H_2O/D_2O reveals a strongly coupled, nonexchangeable proton signal, denoted here as $H_{A/B}$, that has been assigned by Wang et al. in FeS_A to proton(s) of substrate as a result of a comparison of ENDOR spectra from samples prepared with H/D substrate. Figure 9 shows a 2D field-frequency pattern of ^{1}H ENDOR spectra collected across the EPR envelope of FeS_A. Simulations (Figure 9, blue lines) reveal that the ^1H_A signal arises from proton(s) with a nearly isotropic hyperfine coupling, $A(^1H_A) = [14, 11, 11]$ MHz, $a_{iso}(^1H_A) = 12$ MHz. The most strongly coupled nonexchangeable proton in FeS_B, denoted here H_B, has not been assigned. It has a maximum coupling of 11 MHz, and its hyperfine tensor appears to be more anisotropic than that of H_A, although a precise tensor

(51) Stroupe, M. E.; Getzoff, E. D. Sulfite Reductase Hemoprotein. In *Handbook of Metalloproteins*; Messerschmidt, A., Huber, R., Poulos, T., Wieghardt, K., Eds.; John Wiley & Sons, Ltd: Chichester, 2001; pp 471−485.
(52) Wang, W. X.; Li, J. K.; Wang, K.; Huang, C. C.; Zhang, Y.; Oldfield, E. *Proc. Natl. Acad. Sci. U.S.A.* **2010**, *107*, 11189–11193.

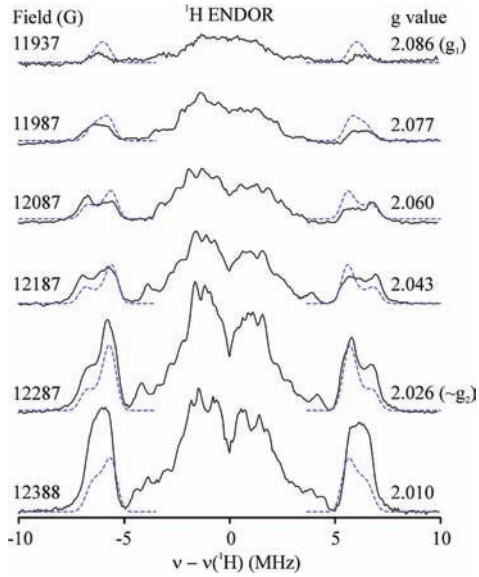

Figure 9. 35 GHz pulsed ^{1}H ENDOR spectra and simulations at 2 K for GcpE samples flash frozen after 10 s incubation time (FeS_A signal). EPR conditions: Davies pulse sequence, microwave π pulse length 200 ns, RF pulse length 20 ms, repetition rate 50 ms, $\tau = 800$ ns, microwave frequency 34.844 GHz. Simulation parameters: $A = [11, 14, 11]$ MHz, $\gamma = 25°$, $\beta = 60°$, $\alpha = 40°$.

determination is not achievable due to its low intensity, anisotropy, and the uncertainty of g values for the multicomponent FeS_B signal. Careful examination of the field-dependence of the ^1H_B signal suggests that it is associated with the minority species with g values at 2.027 and/or 2.010. At lower g values (higher fields), the strongly coupled peaks are visible all the way to the edge of the major EPR species ($g_\perp = 1.984$), indicating that this minor species has a similar value for g_3. This is consistent with the ^{31}P analysis described below and in the Supporting Information.

Exchangeable Protons. ^{2}H Mims ENDOR of a FeS_A sample in D_2O that was quenched at 10 s (not shown) reveals structure superimposed on the featureless matrix deuteron signal centered at the ^{2}H larmor frequency. The maximum coupling occurs at g_2, where the spectrum shows a quadrupole-split doublet of doublets with a hyperfine ^{2}H splitting of 0.52 MHz, corresponding to a ^{1}H coupling of approximately 3.5 MHz. Comparison of the ^{1}H spectra of H_2O/D_2O samples suggests a ^{1}H doublet split by 3.7 MHz in the H_2O sample that is not present in the D_2O sample, supporting the ^{2}H result. This ^{1,2}H coupling is comparable to the 4 MHz exchangeable ^{1}H coupling that is observed in substrate-free aconitase and is associated with a solvent-derived hydroxyl bound to a $[Fe_4S_4]^+$ cluster, and somewhat smaller than that of a hydroxyl of the bound substrate.[53] However, H-bonding to the cluster sulfurs can give exchangeable signals with comparable couplings. Thus, overall, this observation is compatible with an hydroxyl-bound Fe, but not proof of one. Equivalent experiments with samples showing the FeS_B signal yield a similar result, with a 3.8 MHz exchangeable proton observed in the D_2O ^{2}H and H_2O/D_2O ^{1}H difference spectrum at g_3.

^{31}P. Figure 10 shows the ^{31}P-Mims ENDOR data for an EPR sample that was quenched at 10 s and only shows the transient FeS_A signal (Figure S4, Supporting Information). The spectra

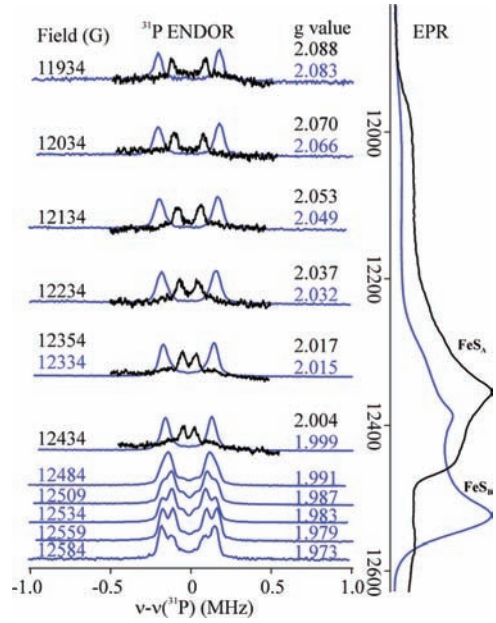

Figure 10. 35 GHz pulsed ^{31}P ENDOR spectra at 2 K of GcpE samples flash frozen after 10 s (FeS_A, black line) and 5 min (FeS_B, blue line) incubation time. Spectra were collected at the fields and g values indicated, and are shown alongside the respective pulse-echo detected EPR spectra. ENDOR spectra are normalized to a fixed intensity for clarity. Conditions: Mims pulse sequence, microwave pulse length 30 ns, RF pulse length 20 μs, repetition rate 20 ms, $\tau = 800$ ns (10 s sample); 500 ns (5 min EPR); 600 ns (5 min ENDOR), microwave frequency 34.857 GHz (5 min); 34.876 GHz (10 s EPR); 34.871 GHz (10 s ENDOR).

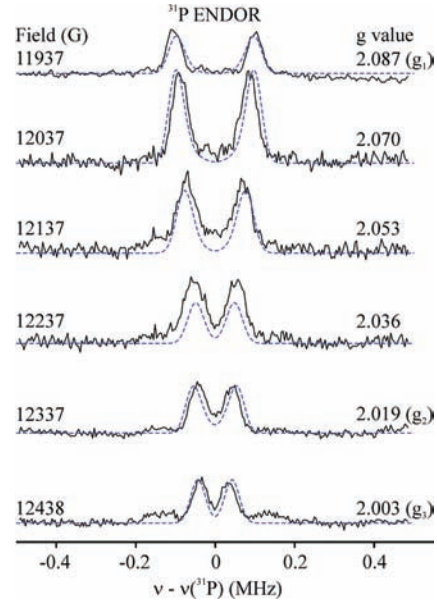

Figure 11. 35 GHz pulsed ^{31}P ENDOR spectra (black line) and dipolar dominated simulation (blue line) for GcpE sample flash frozen after 10 s incubation time (FeS_A signal). EPR conditions as in Figure 10, with $\tau = 600$ ns. Simulation parameters: $A = [0.22, -0.11, -0.09]$ MHz, $\gamma = 20°$.

(Figure 10, black spectra) show a doublet centered at the ^{31}P Larmor frequency with a maximum splitting of about 0.2 MHz at g_1, clearly demonstrating the presence of a single ^{31}P nucleus in proximity to the cluster spin. The data can be simulated using either a dipolar ([0.22, −0.11, −0.09] MHz, Figure 11) or isotropic ([0.21, 0.09, 0.05] MHz, Figure 12) dominated tensor, but regardless of the model, the small size of the coupling

(53) Werst, M. M.; Kennedy, M. C.; Beinert, H.; Hoffman, B. M. *Biochemistry* **1990**, *29*, 10526–10532.

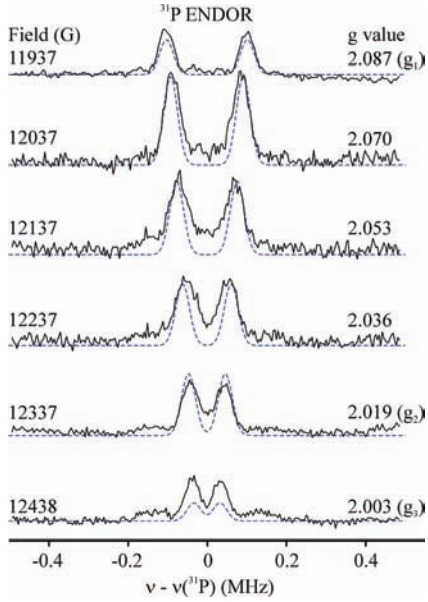

Figure 12. 35 GHz pulsed ^{31}P ENDOR spectra (black line) and isotropic dominated simulations (blue line) for GcpE sample flash frozen after 10 s incubation time (FeS_A signal). EPR conditions as in Figure 10, with τ = 600 ns. Simulation parameters: A = [0.21, 0.09, 0.05] MHz.

indicates that the phosphate groups of MEcPP, although nearby to the cluster associated with the FeS_A signal, are not directly bound to the cluster. The couplings are in fact smaller than observed for the distant, nonbonding phosphate in an intermediate of the enzyme lysine 2,3-aminomutase.[54] Using the same simple point dipole calculation detailed in the previous reference, and treating the iron sulfur cluster as a point source of unit electron spin density, the maximum dipolar tensor above gives a minimum distance of the phosphorus nucleus from the unique iron of 6.6 Å.

Also shown as an overlay in Figure 10 (blue spectra) are the ^{31}P-ENDOR data for a sample that was frozen after 5 min of incubation displaying the mixture of FeS_B signals (Figure S4, Supporting Information). At g_1, a single pair of peaks is observed centered about the ^{31}P Larmor frequency, also with coupling that is small, $A \sim 0.4$ MHz, although larger than that observed for the 10 s FeS_A sample. Thus, the FeS_B centers also have a phosphate group, probably from HMBPP, nearby to the cluster, but this coupling also is too small for direct binding of phosphate to the cluster. Above ~12 300 G, three different ^{31}P features are visible. None correspond to those observed for the 10 s sample, indicating that there is no EPR signal from the FeS_A center in this sample.

Analysis of the multiple ^{31}P features at fields above 12 300 G must take into account the observation, described above, that the EPR spectrum of the 5 min sample shows multiple features due to different species. The bulk of the EPR intensity appears to be due to an axial species with $g_{\|} = 2.081$, $g_{\perp} = 1.984$, while additional features are seen within this range at g values of 2.027 and 2.010 (Figure 7, trace B, and S4). It is not certain whether these features belong to the same EPR species, but their relative intensities remain identical under a range of experimental conditions. While there are no resolved ^{31}P ENDOR features that appear to correspond to the EPR intensity at the latter g values, the overall intensity of the ^{31}P ENDOR increases in approximate proportion to the increase in EPR intensity, indicating that all of the EPR species present (at least two) show ^{31}P ENDOR due to interaction with the product HMBPP. Furthermore, analysis of a second sample (not shown) showed a significantly different intensity ratio for one of the three ENDOR peaks compared to the other two, ruling out the possibility that all three of the ENDOR peaks could arise from the two phosphorus atoms of the substrate and a single EPR species. Because of the presence of an overlapping EPR signal from FeS_A in this second sample, it is difficult to determine whether its FeS_B EPR spectrum was atypical.

Given the uncertainty surrounding the number of EPR species, their g values and the number of contributing ^{31}P nuclei, no definitive fit for the data can be obtained; however, we can account for all the data with any one of the three simplest models, all with maximum observed ^{31}P hyperfine coupling of ~0.4 MHz. A full description of these models and simulations for FeS_B can be found in the Supporting Information (Figures S5−S13). Regardless of the model, the small coupling precludes the direct binding of phosphate to the cluster.

Discussion

Presented is a full EPR/ENDOR spectroscopic characterization of the [4Fe−4S] cluster in GcpE and several paramagnetic species detected in kinetic studies. We propose that the cluster plays an important role in substrate binding and catalysis. One of the points addressed is the role of the reduced form of the cluster in the reaction mechanism. This is of particular importance since reduction with dithionite in the absence of substrate resulted in only partial reduction of the cluster in the *T. thermophilus* enzyme. The maximal amount of reduction was only 0.05 spin. Reduction with the more potent reductant Ti(III) citrate not only results in cluster reduction but also in cluster breakdown. The complete breakdown of the cluster can be prevented when substrate is added to the enzyme solution. Still, there is a small redox-potential window where the enzyme can work optimally. Above a certain potential, there is not enough reductive power to get the reaction started or to get past the first reaction intermediate. Below a certain potential, the protein becomes more vulnerable to cluster breakdown. This is in line with the work by Liu and co-workers where the highest enzyme activity was detected at a potential of −446 mV (vs NHE).[48] Using reductants with lower potential did not increase the activity any further but instead a decrease was observed. From a mechanistic perspective, however, having a reduced cluster donating electrons to the substrate would make sense. This is supported by the work shown in Figure 5. In this experiment, the only reductant present in the enzyme solution is the reduced 4Fe cluster itself. Addition of MEcPP resulted in the formation of the FeS_A species, indicating that the formation of this intermediate does not require added electrons.

It is also clear from the work presented here that there are different midpoint potentials associated with different steps of the reaction mechanism. When the dithionite concentration is kept below 10 mM only one species, denoted FeS_A, accumulates during substrate turnover. Above 10 mM a full reaction takes place in line with previous work that showed that only dithionite is needed for product formation.[25] Unfortunately, obtaining kinetic parameters like V_{max} and K_M using a kinetic assay with only dithionite is not possible due to the high concentration of dithionite needed. In addition, the detection of product formation using for example NMR spectroscopy is not possible due to detection limits (product inhibition will occur before enough

(54) Lees, N. S.; Chen, D. W.; Walsby, C. J.; Behshad, E.; Frey, P. A.; Hoffman, B. M. *J. Am. Chem. Soc.* **2006**, *128*, 10145–10154.

product has accumulated). In future work, the redox potentials under the different reaction conditions have to be measured to get a complete picture of the redox potential dependency of the different reaction steps in GcpE. In addition, there has to be a difference in how the different reductants used in this study interact with GcpE. With reduced methyl viologen or mixtures of dithionite and methyl viologen, a faster reaction rate is observed, although the redox potential of these compound and/or mixtures is not that different. The fact that reduced methyl viologen is positively charged and dithionite is negatively charged could explain a difference in interaction of these compounds with the enzyme and/or cluster. It appears that dithionite can provide electrons for the second step with more difficulty. If the cluster is present in an active-site channel, it could be that the binding of substrate to the cluster limits the access of dithionite to the cluster.

With mixtures of dithionite and methyl viologen, no or very small amounts of the FeS_A species were detected in EPR spectroscopy, but a second group of signals, denoted FeS_B, started to accumulate within 10 s of incubation time, which is within the 11 s calculated for a full reaction cycle. This would indicate that in the presence of methyl viologen the breakdown of the species represented by the FeS_A EPR signal is not the rate limiting step as it appears to be the case when only dithionite is present.

There are three known classes of proteins that have a 4Fe cluster that is directly involved in catalysis. The first class is the hydrolyase class with aconitase as a prominent member.[55,56] The dehydration reactions catalyzed by this class of enzymes do not involve redox chemistry. Substrates coordinate to a $[4Fe-4S]^{2+}$ cluster at the so-called unique iron site, which is the iron that is not coordinated by the sulfur atom of a cysteine residue. The $[4Fe-4S]^{2+}$ cluster serves as a Lewis acid to facilitate dehydration to form a C=C double bound and rehydration of it.[55,56] In the case of aconitase, the substrate citrate is bound to the unique iron via one of the oxygen atoms from a carboxyl group and one oxygen atom from a hydroxyl group. The coordination makes the hydroxyl group a better leaving group. The second class is represented by the radical SAM enzymes that function in DNA repair, and the biosynthesis of vitamins, coenzymes, and antibiotics.[57−60] The common thread in the function of these enzymes is the use of a strong reducing agent, a low potential $[4Fe-4S]^{+}$ cluster, to generate a powerful oxidizing agent, the 5′-deoxyadenosyl radical by reductive cleavage of S-adenosylmethionine (SAM). For this to happen, SAM coordinates to the unique iron of the cluster via its amino and carboxylate groups.[58,61] The third class known to date consists of only two proteins: ferredoxin:thioredoxin reductase (FTR)[34−38] and heterodisulfide reductase.[49,62,63] FTR functions as a switch, using single electrons donated by ferredoxin for a two-electron reduction of a disulfide bond present on the substrate thioredoxin. The active site of FTR contains the unique combination of a [4Fe−4S] cluster in close proximity to an active-site disulfide bond.[64] Transfer of the first electron from the $[4Fe-4S]^{+}$ cluster to the disulfide would in principle cause the formation of a thiolate and a thiyl radical. The formation of the radical species, however, is prevented by forming a bond between this sulfur atom and an iron atom of the 4Fe cluster. The unique iron site ends up being coordinated by two cysteinates. This species is best described as a $[4Fe-4S]^{3+}$ cluster and shows the unusual electronic and magnetic properties and temperature behavior described.

How does GcpE fit into these three groups? The data presented here show that in kinetic studies a transient paramagnetic species is detected in GcpE that has EPR properties that are remarkably similar to that detected in FTR, which indicates that a reaction intermediate could be bound to a $[4Fe-4S]^{3+}$ cluster. In this case, the leaving hydroxyl group of MEcPP is the most likely candidate to coordinate to the cluster as small ^{31}P hyperfine couplings measured for the FeS_A and FeS_B intermediates appear to exclude direct phosphate binding to the cluster, unless the vector-coupling coefficient to the unique Fe is anomalously small. It is important to note that the next enzyme in the MEP pathway, the LytB (or IspH) enzyme, catalyzes a very similar reductive elimination of a hydroxyl group. LytB also appears to contain a [4Fe−4S] center that has been proposed to directly bind the substrate or a reaction intermediate. Moreover, a recent crystal structure showed the substrate HMBPP to be within the active site, bound to the 4Fe cluster via its hydroxyl group.[65] However, ENDOR measurements led to the proposal that HMBPP, or a reaction intermediate, binds to the cluster of LytB, as a π and/or η complex,[66] a proposal based on analogy to the original discovery of such an organometallic intermediate in catalysis by nitrogenase.[67]

Not all the mechanistic details of GcpE catalysis are clear at this point, but it is clear that the iron−sulfur cluster has an important function. Both FeS_A and FeS_B have an average g value $> g_e$, which is strongly indicative of a $[4Fe-4S]^{3+}$ species.[68,69] On the basis of the similarities of both the g values and EPR properties with the EPR signal detected in FTR, the FeS_A signal could be assigned to a substrate-bound $[4Fe-4S]^{3+}$ species.[38] However, the FeS_B signal that can be induced not only under turnover conditions, but also by binding of product HMBPP to the reduced $[4Fe-4S]^{1+}$ cluster, and therefore almost certainly involves a +1 cluster, has similarities to that of the FeS_A species. The g values of FeS_B are more "+1-like", with $g_\perp < g_e$, in contrast to FeS_A where $g_{xyz} \geq g_e$, but FeS_B nonetheless has $g_{av} > g_e$, which is highly unusual for a $[4Fe-4S]^{1+}$ species. This raises the possibility that FeS_A is also a $[4Fe-4S]^{1+}$ species, despite the highly suggestive g values. Mössbauer spectroscopy studies will be needed to address the oxidation state of the [4Fe−4S] cluster in the FeS_A form.

(55) Flint, D. H.; Allen, R. M. *Chem. Rev.* **1996**, *97*, 2315–2334.
(56) Beinert, H.; Kennedy, M. C.; Stout, C. D. *Chem. Rev.* **1996**, *97*, 2315–2334.
(57) Sofia, H. J.; Chen, G.; Hetzler, B. G.; Reyes-Spindola, J. F.; Miller, N. E. *Nucleic Acid Res.* **2001**, *29*, 1097–1106.
(58) Layer, G.; Heinz, D. W.; Jahn, D.; Schubert, W.-D. *Curr. Opin. Chem. Biol.* **2004**, *8*, 468–476.
(59) Marsh, E. N. G.; Patwardhan, A.; Huhta, M. S. *Bioorg. Chem.* **2004**, *32*, 326–340.
(60) Wang, S. C.; Frey, P. A. *Trends Biochem. Sci.* **2007**, *32*, 101–110.
(61) Berkovitch, F.; Nicolet, Y.; Wan, J. T.; Jarrett, J. T.; Drennan, C. L. *Science* **2004**, *303*, 76–79.
(62) Madadi-Kahkesh, S.; Duin, E. C.; Heim, S.; Albracht, S. P. J.; Johnson, M. K.; Hedderich, R. *Eur. J. Biochem.* **2001**, *268*, 2566–2577.
(63) Duin, E. C.; Bauer, C.; Jaun, B.; Hedderich, R. *FEBS Lett.* **2003**, *538*, 81–84.
(64) Dai, S.; Saarinen, M.; Ramaswamy, S.; Meyer, Y.; Jacquot, J.-P.; Eklund, H. *J. Mol. Biol.* **1996**, *264*, 1044–1057.
(65) Gräwert, T.; Span, I.; Eisenreich, W.; Rohdich, F.; Eppinger, J.; Bacher, A.; Groll, M. *Proc. Natl. Acad. Sci. U.S.A.* **2010**, *107*, 1077–1081.
(66) Wang, W. X.; Wang, K.; Liu, Y. L.; No, J. H.; Li, J. K.; Nilges, M. J.; Oldfield, E. *Proc. Natl. Acad. Sci. U.S.A.* **2010**, *107*, 4522–4527.
(67) Lee, H. I.; Igarashi, R. Y.; Laryukhin, M.; Doan, P. E.; Dos Santos, P. C.; Dean, D. R.; Seefeldt, L. C.; Hoffman, B. M. *J. Am. Chem. Soc.* **2004**, *126*, 9563–9569.
(68) Mouesca, J. M.; Lamotte, B. *Coord. Chem. Rev.* **1998**, *178*, 1573–1614.
(69) Lepape, L.; Lamotte, B.; Mouesca, J. M.; Rius, G. *J. Am. Chem. Soc.* **1997**, *119*, 9757–9770.

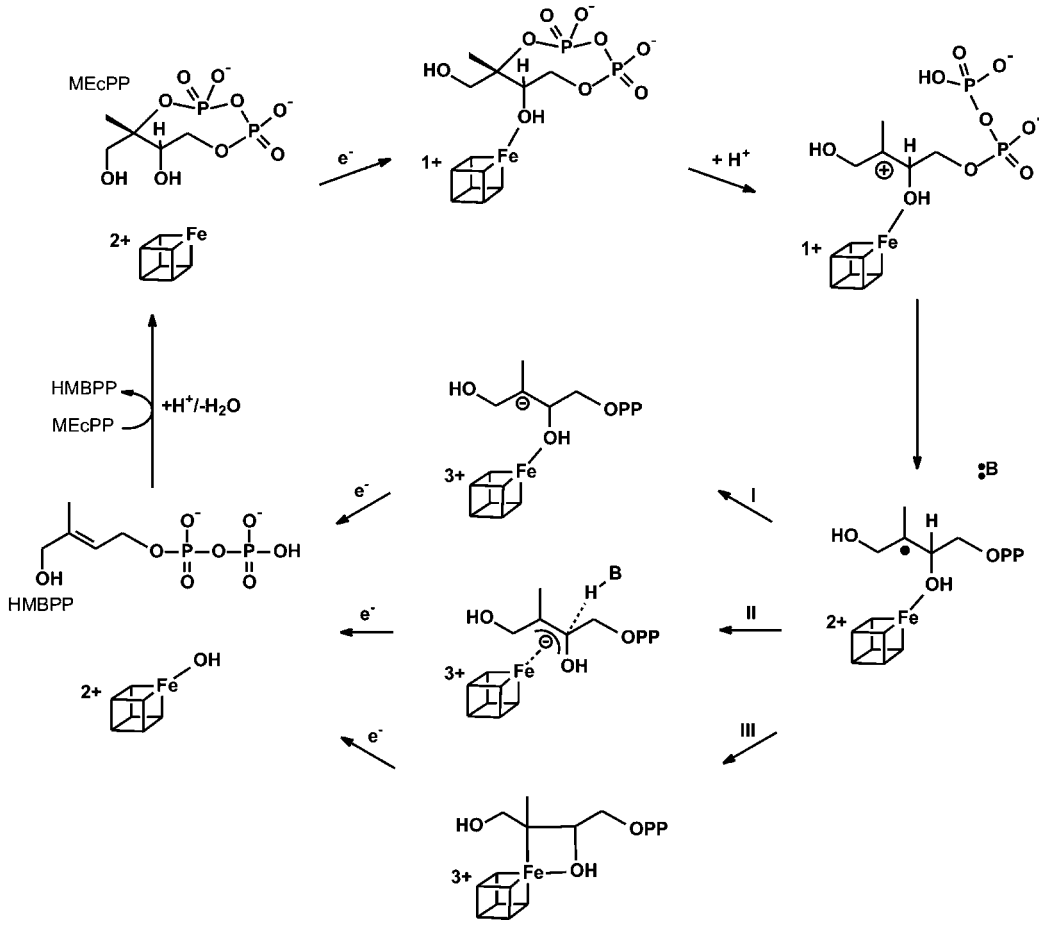

Figure 13. Hypothetical reaction mechanism for GcpE. See text for detailed description.

The recent study by Wang et al. of GcpE first reported the ENDOR signal from H_A, and demonstrated that it was associated with a substrate-derived moiety bound to the cluster through use of isotopically labeled substrate.[52] In that report, H_A was assigned to the α proton of C3, which was bound to Fe as part of a ferraoxetane ring. However, the H_A hyperfine tensor was not determined. The present determination that the hyperfine coupling to H_A is nearly isotropic raises a question about the earlier assignment. A proton bound to a first-row atom coordinated to a metal ion has been observed to have a highly anisotropic coupling, in contrast to the coupling for H_A.[70]

The driving force for the proposal of a ferraoxetane structure was the observation of a large ^{13}C coupling assigned to C3, $A = 19$ MHz (no tensor determined). While this is indeed suggestive, we note that the formaldehyde-inhibited form of the molybdo-enzyme, xanthine oxidase, exhibits a ^{13}C coupling of $a_{iso} = 43$ MHz for a moiety derived from formaldehyde, yet it was recently shown that this carbon is not bonded to the metal ion, but rather the observed coupling reflected a large "transannular" hyperfine interaction associated with a carbon not bonded to the metal ion but part of a four-membered metallacycle.[71] This observation, plus the near-isotropy of the H_A coupling, suggests that *if* the ferraoxetane structure proposed by Wang et al. is correct, a plausible assignment might instead be that H_A represents protons on the methyl group and/or protons on C1, and that the strongly coupled carbon is C2. These alternatives would be readily distinguished with selective isotopic labeling. Alternatively, a ferraoxetane with an Fe−C2 bond (Figure 13), also considered by Wang et al., although not favored, might be expected to have a large coupling to $^{13}C3$ and its α proton, and thus this assignment probably is to be preferred.

For completeness, we note that the rather large H_A coupling is not on its face evidence for assignment to a structure with a metal−carbon bond. In the case of allylbenzene-inactivated chloroperoxidase (AB-CPO), the proton of the Fe(III)−O−C2H- linkage to the low-spin ferriheme exhibits a mostly isotropic coupling that is considerably larger than that of H_A: $\mathbf{A}(H) = [24.6, 17.0, 16.2]$ MHz, $a_{iso}(H) = 19.3$ MHz[72] compared to $a_{iso}(H_A) = 12$ MHz. However, in AB-CPO, the maximum coupling, to $^{13}C2$, was only A ∼5 MHz. Whether a larger coupling might arise with a high-spin Fe ion embedded in a cluster would require further experimental study and/or electronic-structure computations.

In the hypothetical mechanism proposed in Figure 13, it is assumed that the reaction begins with the binding of MEcPP to GcpE containing a $[4Fe-4S]^{2+}$ cluster. This results in a change in midpoint potential of the cluster and its reduction by electron transfer from dithionite, or in the cell by the natural electron donor. This species is one of the candidates for the origin of the FeS_A signal (1+ form). However, it is not clear why this

(70) Lees, N. S.; McNaughton, R. L.; Gregory, W. V.; Holland, P. L.; Hoffman, B. M. *J. Am. Chem. Soc.* **2008**, *130*, 546–555.
(71) Shanmugam, M.; Zhang, B.; McNaughton, R. L.; Hille, R.; Hoffman, B. M. *J. Am. Chem. Soc.* **2010**, in press.
(72) Lee, H. I.; Dexter, A. F.; Fann, Y. C.; Lakner, F. J.; Hager, L. P.; Hoffman, B. M. *J. Am. Chem. Soc.* **1997**, *119*, 4059–4069.

species should accumulate in any significant amounts. Protonation of MEcPP results in ring-opening and the formation of a carbocation. Internal electron transfer from the cluster to the substrate results in the formation of a carbon radical. There are several possibilities of how the cluster can stabilize this radical species. One option would be the transfer of an additional electron, making the cluster formally 3+ (reaction I). Such a species would be the second candidate for the origin of the FeS_A species. However, this would create a carbanion species that could be very reactive. The ferraoxetane structure as proposed by Wang et al. would provide a way to stabilize the carbanion (and even the radical species in the previous step) by forming an additional bond to the unique iron (via reaction III). Note that the structure does not indicate the preference for a specific orientation of the bound compound. At this point it is not clear, however, if there is a direct bond between the C3 carbon and the unique iron. As an alternative (reaction II) a π/η-type complex can be proposed, perhaps accompanied by interaction with the hydroxyl oxygen. A similar interaction was also proposed for the IspH/LytB enzyme.[66] This type of interaction would require a reversible deprotonation of the C3 carbon. Transfer of the second electron from the outside electron donor to the active-site cluster results in the release of the hydroxyl group and double bond formation. The hydroxyl group can stay bound to the cluster and comes off later since it is only weakly bound as shown for example for aconitase.[56]

The freeze-quench studies (Figure 2) show the formation of a radical species early in the reaction, 28 ms to 0.5 s. It is not clear, however, if this is due to a carbon-based radical-type reaction intermediate or due to dithionite itself. The formation of the FeS_B signals would be due to the adventitious binding of the reaction product HMBPP to the reduced cluster, possibly via the remaining hydroxyl group. It is possible that the multiplicity of species always observed in the FeS_B spectrum, with invariant relative intensity and identical relaxation behavior, is due to different binding modes for HMBPP. An alternative explanation would be that the different signals can be assigned as valence isomers. These are states of a cluster that differ only in the location and pairing of the $Fe^{2+/3+}$ ions. As observed in EPR spectra of other FeS clusters, these result in extra peaks very similar to those observed in FeS_B.[73] One could then suggest that the temperature-dependent collapse of the EPR spectrum is associated with activated exchange among the isomers. We note that such isomers are much more common among $[4Fe-4S]^{3+}$ clusters than among $[4Fe-4S]^{1+}$ clusters.

It has been proposed that an epoxy intermediate is formed in the reaction mechanism.[28] It was recently shown that this epoxy compound is indeed a substrate for GcpE.[74] Without the involvement of an iron−sulfur cluster, an epoxy intermediate might be a necessary reaction step. There is no need, however, to invoke such an intermediate when MEcPP can bind to the unique iron of the 4Fe cluster. Our model is still in line with the epoxy compound being a substrate. Binding of the epoxy compound and simultaneous electron transfer from the cluster would create the same cluster-bound carbon radical species as proposed in Figure 13.

In this paper, we presented a full spectroscopic characterization of the paramagnetic species detected in GcpE during the kinetic experiments. It is clear that the active-site 4Fe cluster plays a very important role in both substrate binding and catalysis. Several possible mechanisms were discussed. Each mechanism has different implications for the type of compounds that could function in inhibiting the GcpE enzyme. It is important to further narrow down these possibilities since the GcpE enzyme is a putative target for the treatment of a wide range of infectious diseases, and detailed knowledge of the actual mechanism will help in finding the correct inhibitor that would be a potential drug candidate.

Acknowledgment. We thank Dr. Boi Hanh Huynh at Emory University, Atlanta, GA, for providing access to his rapid-mix rapid-freeze set up and Dr. Sunil Naik for his assistance with the preparation of the freeze-quench samples. We also thank the group of Dr. Dmitry N. Ostrovsky at the Bakh Institute of Biochemistry, Moscow, Russia, for providing MEcPP.

Supporting Information Available: Kinetic study with equimolar amount of substrate. Temperature behavior of the FeS_A and FeS_B EPR signals. CW EPR spectra of samples studied in ENDOR spectroscopy. Simulations of ^{31}P ENDOR data. This material is available free of charge via the Internet at http://pubs.acs.org.

JA101764W

(73) Priem, A. H.; Klaassen, A. A. K.; Reijerse, E. J.; Meyer, T. E.; Luchinat, C.; Capozzi, F.; Dunham, W. R.; Hagen, W. R. *J. Biol. Inorg. Chem.* **2005**, *10*, 417–424.

(74) Nyland, R. L.; Xiao, Y.; Liu, P.; Freel Meyers, C. L. *J. Am. Chem. Soc.* **2009**, *131*, 17734–17735.